International Journal of Heat and Mass Transfer 216 (2023) 124532

Contents lists available at ScienceDirect

International Journal of Heat and Mass Transfer

journal homepage: www.elsevier.com/locate/ijhmt

# The onset of penetrative convection in an inclined porous layer

Giuseppe Arnone [a], Giulio Cantini [b,c], Florinda Capone [a,*], Mauro Carnevale [b,c]

[a] Dipartimento di Matematica e Applicazioni 'R.Caccioppoli', Università degli Studi di Napoli Federico II, Via Cintia, Monte S.Angelo, Naples, 80126, Naples, Italy
[b] Department of Mechanical Engineering, University of Bath, Claverton Down, Bath, BA2 7AY, Bath, United Kingdom
[c] CERN, Geneva, Switzerland

ARTICLE INFO

*MSC:*
76E06
76Exx
76S05
76Sxx

*Keywords:*
Penetrative convection
Inclined layer
Porous media
Instability analysis
Nonlinear stability
Chebyshev-tau method

ABSTRACT

In the present article, a model for penetrative convection in a fluid-saturated inclined porous medium is analyzed. Penetrative convection occurs when an unstably stratified fluid moves into a stably stratified region. In this study, it will be shown that the inclination of the layer plays a relevant role for the penetrative thermal convection of a fluid-saturated porous medium. The results reported in the literature for the limiting case of horizontal layer are recovered and the numerical results for the linear instability, obtained via the Chebyshev-$\tau$ method, show that the most destabilizing perturbations are the longitudinal and, as expected, the transverse ones destabilize only up to a certain critical inclination angle of the layer. Moreover, in the numerical analysis of the three-dimensional perturbations, we show that the longitudinal perturbations are the most destabilizing not only with respect to the transverse but also with respect to any general perturbation. We also give nonlinear stability results for the longitudinal perturbations via the weighted energy method.

## 1. Introduction

Thermal instability of both clear fluids and fluid-saturated porous layers is a subject that has attracted much attention and has been investigated by many authors because of its numerous and remarkable applications (for a comprehensive problem framing, historical development, and applications see [1–3, and references therein]). There are essentially two typical situations bringing thermal instability. The first is the heating from below mechanism, which is the phenomenon responsible for the activation of the so-called *Rayleigh-Bénard convection* in a clear fluid at rest (see [1,4]). The corresponding mathematical problem, called the Bénard Problem after Henry Bénard [5], whose crucial experimental investigations represent a milestone, was solved by Lord Rayleigh in 1916 [6]. Concerning fluid-saturated porous media, the Rayleigh-Bénard instability yields the formulation of the Horton-Rogers-Lapwood problem [7,8], and the specific interests for geophysical applications were highlighted in pioneering papers as those by Wooding [9] and Elder [10]. The second typical situation occurs when the fluid density attains a maximum in the interior of the porous layer. In this case, the process of thermal convection refers to the instability of a part of the layer, which will then penetrate into an upper stability-stratified region. This density inversion phenomenon, see [11], is indeed responsible for the activation of the so-called *penetrative convection*. The mathematical formulation of this problem was addressed for the first time by Veronis [12]. Since then, considerable attention has been devoted to penetrative convection, in both frameworks of clear fluids [13,14] and porous media [15,16]; the latter, especially for its applications in geophysics [17,18]. In particular, in [13] the case of isothermal boundaries was considered, while in [14] the case of a given heat flux was investigated. Among all physical setups, the inclination of the layer plays a relevant role in the thermal convection of fluid-saturated porous medium, and it applies in many environmental circumstances. In this regard, it has been noticed that thermal convection has a role in the diffusion of pollutants in the underground [19,20] or in land deformation involving thermal gradient, see [21, and references therein]. Because of the aforementioned applications both experimental [22,23] and theoretical studies [24–30] have been conducted in recent years. The novelty of the present research is the development, as far as we know for the first time, of a theoretical investigation of penetrative convection in a fluid-saturated inclined porous medium, by assuming the validity of Darcy's law [2,31]. The authors addressed the present study with the aim of a deep understanding of

* Corresponding author.
*E-mail address:* fcapone@unina.it (F. Capone).

https://doi.org/10.1016/j.ijheatmasstransfer.2023.124532
Received 14 April 2023; Received in revised form 20 July 2023; Accepted 20 July 2023
Available online 3 August 2023
0017-9310/© 2023 The Author(s). Published by Elsevier Ltd. This is an open access article under the CC BY-NC-ND license (http://creativecommons.org/licenses/by-nc-nd/4.0/).

the combined mechanism of penetrative convection and inclination of the porous layer, which gives an explanation of several phenomena like patterned ground formations [17] and thawing subsea permafrost [18]. The dimensionless governing parameter that describes the onset of thermal convection is the Darcy-Rayleigh number, Ra. This parameter marks the *threshold* for the onset of convection. Namely, in the linear regime, a critical value $\mathsf{Ra}_L$, such that thermal convection occurs for higher values of Ra, can be determined. Concerning the nonlinear stability analysis, the conditions for which a suitable energy functional is decreasing along the solution of the system (one usually refers to this methodology as the *Lyapunov method*, or *energy method*, see [32,31,33]) give rise a critical value $\mathsf{Ra}_E (\leq \mathsf{Ra}_L)$ below which the conduction solution is asymptotically exponentially stable, i.e. we will not observe the onset of convection. The choice of a suitable energy functional is crucial for the nonlinear analysis and it is a delicate matter addressed by many authors, see e.g. [34–38]. Here we study the linear instability of the conduction solution for longitudinal (also called streamwise), transverse (also called spanwise), and full three-dimensional perturbations and the nonlinear stability analysis with respect to the longitudinal ones. In particular, the numerical results for the linear instability, obtained via the Chebyshev-$\tau$ method, show that the most destabilizing perturbations are the longitudinal ones and, as expected, the transverse ones exhibit a peculiar phenomenon: they destabilize only up to a certain critical inclination angle of the layer. This means, in other words, that above this critical angle, there will be a preferred orientation for the perturbations at the onset of the secondary flow. Indeed, from the numerical analysis of the three-dimensional perturbations, we show that the spanwise ones are the most destabilizing not only with respect to the streamwise but also with respect to any general roll perturbation. Hence, this numerically shows the validity of a Squire-like theorem [39–41]. Summing up, the paper is organized as follows. In Section 2 the mathematical model is introduced and the Darcy-Rayleigh number is defined in the non-dimensional framework. Then, the steady-state solution is computed and the perturbed non-dimensional system is derived. Section 3 deals with the linear instability analysis. In particular, the longitudinal and transverse perturbations cases are analyzed separately. Moreover, for the former case, the *principle of exchange of stabilities* is proved and the linear critical Rayleigh numbers, for the onset of steady convection are found to be the same as those for the horizontal layer up to a scaling factor. In Section 4 we give some nonlinear stability results of the longitudinal perturbations. More specifically, by introducing a suitable Lyapunov functional, we find the non-linear critical Rayleigh numbers be solving the Euler-Lagrange equations arising from a maximum problem. In Section 5, the employed numerical method (Chebyshev-$\tau$) is explained, and the paper ends with a concluding Section 6 in which all the numerical results are shown and commented on and the obtained results are summarized.

**Nomenclature**

| Symbol | Unit | Description |
|---|---|---|
| $d$ | $m$ | depth of the layer |
| $t$ | $s$ | time |
| $T_L$ | $K$ | lower temperature |
| $T_U$ | $K$ | upper temperature |
| $T_0$ | $K$ | reference temperature |
| $\mu$ | $kg/(m\,s)$ | dynamic fluid viscosity |
| $\rho$ | $kg/m^3$ | fluid density |
| $\alpha$ | $K^{-2}$ | thermal expansion coefficient |
| $g$ | $m/s^2$ | modulus of gravitational acceleration |
| $k$ | $m^2$ | permeability of the porous body |
| $\kappa$ | $m^2/s$ | thermal diffusivity |
| $p$ | $Pa$ | pressure field |
| $\mathbf{v}$ | $m/s$ | seepage velocity |
| $T$ | $K$ | temperature field |
| $\varphi$ | | layer inclination |
| Ra | | Rayleigh-Darcy number |

## 2. Formulation of the problem

### 2.1. Matematical model

Let $Oxyz$ be a Cartesian reference frame with fundamental unit vector $\mathbf{i},\mathbf{j},\mathbf{k}$ (the latter pointing vertically upwards) and let $L$ be an isotropic porous medium with thickness $d > 0$, inclined of an angle $\varphi \in \left[0, \frac{\pi}{2}\right]$ with respect to the horizontal plane. The layer $L$ is saturated by a homogeneous incompressible Newtonian fluid confined between two parallel impermeable planes kept at uniform and constant temperatures $T_L$ and $T_U$. As stated in the introduction, penetrative convection can occur when the fluid density attains a maximum in the interior of the porous layer and this is possible when the density of the fluid has the following quadratic dependence on the temperature [12]:

$$\rho(T) = \rho_0[1 - \alpha(T - T_0)^2], \tag{1}$$

where $\rho_0 = \rho_0(T_0)$ is a reference density at a reference temperature $T_0$ and $\alpha$ is the thermal expansion coefficient. Among all fluids, water exhibits this anomalous density-temperature relation, being near parabolic around $4°C$. In particular, see [12], the quadratic dependence (1), with $T_0 = 4°C$, $\rho_0$ density of water at the density inversion point and $\alpha \simeq 7.68 \times 10^{-6}/(°C^2)$, accurately represent the water's density in its parabolic neighborhood and involves a 10% error at $14°C$. In this paper, the above physical setup is assumed. We must emphasize the fact that perfectly incompressible media do not exist in nature. Nonetheless, they can be considered as a limit case of compressible one. Assuming as definition of incompressibility the independence of the constitutive equations from the pressure, Müller [42] proved that this definition is compatible with the entropy principle only if the density is a constant function. This statement, usually called *Müller paradox*, is in disagreement with empirical observations, according to which fluids expand when heated, and the widely employed Boussinesq approximation, see [2,32]. Gouin et al., in [43] fixed this contradiction introducing the definition of *quasi-thermal-incompressible fluids*: media for which the density is the *only* equation independent of the pressure among all the constitutive equations. Employing this definition the authors proved that a quasi-thermal-incompressible fluid *tends* to be perfectly incompressible when $p \ll p_{cr}$, being $p_{cr}$ a critical pressure value below which the incompressibility assumption is thermodynamically consistent. The critical pressure value for the penetrative convection problem can be found in [16]. We assume that Darcy's law models the momentum balance equation and we adopt the Boussinesq approximation scheme and the Veronis density law (1), namely:

$$\frac{\mu}{k}\mathbf{v} = -\nabla p - g\rho(T)\mathbf{r}, \tag{2}$$

where $\mathbf{v}$, $p$ and $\rho$ are the seepage velocity, pressure and density respectively, $\mathbf{r} = (\sin\varphi, 0, \cos\varphi)^T$, $g$ is the modulus of gravitational acceleration, $\mu$ is the dynamic viscosity and $k$ the permeability of the porous medium. Equation (2), together with the mass conservation law and the energy balance equation governing the behavior of the temperature field in local thermal equilibrium, yields the following system of governing equations:

$$\begin{cases} \dfrac{\mu}{k}\mathbf{v} = -\nabla\tilde{p} - 2g\rho_0\alpha T_0 T\mathbf{r} + g\rho_0\alpha T^2\mathbf{r}, \\ \nabla\cdot\mathbf{v} = 0, \\ \dfrac{\partial T}{\partial t} + \mathbf{v}\cdot\nabla T = \kappa\Delta T, \end{cases} \tag{3}$$

where $\kappa$ is the thermal diffusivity and

$$\tilde{p} = p + g\rho_0(1 - \alpha T_0^2)(x\sin\varphi + z\cos\varphi). \tag{4}$$

For the sake of brevity, but without loss of generality, we omit the tilde on the pressure function $p$. We complete system (3) with the following boundary conditions:

$$T(x,y,0,t)=T_L, \quad T(x,y,d,t)=T_U, \tag{5}$$

and

$$\mathbf{v}\cdot\mathbf{n}=0 \quad \textbf{on} \quad z=0,d, \tag{6}$$

where $\mathbf{n}$ is the unit outward normal to the planes bounding the layer. In particular, for the problem under examination, we assume:

$$T_L=0°C, \quad T_0=4°C, \quad T_U\geq 4°C. \tag{7}$$

### 2.2. Steady state solution and perturbation equations

In order to rewrite the system (3) in non-dimensional form let us introduce the following non-dimensional parameters:

$$\mathbf{x}=d\mathbf{x}^*, \quad t=\tau t^*, \quad \mathbf{v}=V\mathbf{v}^*, \quad p=Pp^*, \quad T=T_UT^*, \tag{8}$$

with

$$\tau=\frac{d^2}{\kappa}, \quad V=\frac{\kappa}{d}, \quad P=\frac{\mu\kappa}{k}. \tag{9}$$

Then the resulting non-dimensional equations of motion, omitting all the asterisks, are the following:

$$\begin{cases} \mathbf{v}=-\nabla p-\mathsf{Ra}\left(\zeta T-\dfrac{T^2}{2}\right)\mathbf{r}, \\ \nabla\cdot\mathbf{v}=0, \\ \dfrac{\partial T}{\partial t}+\mathbf{v}\cdot\nabla T=\Delta T, \end{cases} \tag{10}$$

where the dimensionless parameter $\mathsf{Ra}$ (the thermal Darcy-Rayleigh number) and $\zeta$ are respectively given by:

$$\mathsf{Ra}=\frac{2g\rho_0\alpha k d T_U^2}{\mu\kappa}, \qquad \zeta=\frac{T_0}{T_U}. \tag{11}$$

Note that the boundary conditions on the temperature, in the non-dimensional framework, are the following:

$$T(x,y,0,t)=0, \quad T(x,y,1,t)=1. \tag{12}$$

We now seek stationary and laminar basic solutions

$$m_b=(\mathbf{v}_b,p_b,T_b), \tag{13}$$

with $\mathbf{v}_b=(v_b(z),0,0)$, whose instability and stability are going to be the core of the present investigations. From $(10)_3$ one easily finds:

$$T_b(z)=z. \tag{14}$$

By substituting (14) in $(10)_1$ we obtain

$$\begin{aligned} v_b(z)&=-\frac{\partial p_b}{\partial x}-\mathsf{Ra}\left(\zeta z-\frac{z^2}{2}\right)\sin\varphi, \\ 0&=-\frac{\partial p_b}{\partial y}, \\ 0&=-\frac{\partial p_b}{\partial z}-\mathsf{Ra}\left(\zeta z-\frac{z^2}{2}\right)\cos\varphi. \end{aligned} \tag{15}$$

Moreover, from equations $(15)_{2,3}$ it follows that

$$p_b=p_b(x,z)=g(x)-\mathsf{Ra}\left(\zeta\frac{z^2}{2}-\frac{z^3}{6}\right)\cos\varphi, \tag{16}$$

and substituting in $(15)_1$ we have

$$v_b(z)+\mathsf{Ra}\left(\zeta z-\frac{z^2}{2}\right)\sin\varphi=-\frac{d}{dx}g(x). \tag{17}$$

The previous ordinary differential equation must be satisfied identically in $\mathbb{R}\times[0,1]$. As a consequence, that there exist a constant $\eta$, a pressure gradient along $x$ and a constant $c$, see [27], such that

$$g(x)=\eta x+c. \tag{18}$$

Hence

$$v_b(z)+\mathsf{Ra}\left(\zeta z-\frac{z^2}{2}\right)\sin\varphi=-\eta. \tag{19}$$

For simplicity we set $\eta=0$, and, recalling (4), we have

$$p_b(x,z)=C-\mathsf{Ra}\left(\zeta\frac{z^2}{2}-\frac{z^3}{6}\right)\cos\varphi-A(1-\alpha T_0^2)(x\sin\varphi+z\cos\varphi), \tag{20}$$

with $A=\frac{g\rho_0 dk}{\mu\kappa}$ a non-dimensional constant. Therefore, the complete steady state solution is fully computed

$$\begin{aligned} m_b=\Big(&\Big(-\mathsf{Ra}\Big(\zeta z-\frac{z^2}{2}\Big)\sin\varphi,0,0\Big), \\ &c-\mathsf{Ra}\Big(\zeta\frac{z^2}{2}-\frac{z^3}{6}\Big)-A(1-\alpha T_0^2)(x\sin\varphi+z\cos\varphi),z\Big). \end{aligned} \tag{21}$$

Note that if $\varphi=0$, $m_b$ coincides with the steady state motion for penetrative convection in a horizontal layer found in [16].

In order to study the stability of $m_b$, we introduce the following perturbation fields

$$\mathbf{v}=\mathbf{v}_b+\mathbf{u}, \quad p=p_b+\pi, \quad T=T_b+\theta, \tag{22}$$

with $\mathbf{u}=(u,v,w)$. Eventually, the resulting non-dimensional perturbation equations are

$$\begin{cases} \mathbf{u}=-\nabla\pi-\mathsf{Ra}M(z)\theta\mathbf{r}+\dfrac{\mathsf{Ra}}{2}\theta^2\mathbf{r}, \\ \nabla\cdot\mathbf{u}=0, \\ \dfrac{\partial\theta}{\partial t}+v_b(z)\theta_x+w+\mathbf{u}\cdot\nabla\theta=\Delta\theta, \end{cases} \tag{23}$$

with $M(z)=\zeta-z$, together with initial conditions

$$\mathbf{u}(\mathbf{x},t_0)=\mathbf{u}_0(\mathbf{x}), \quad \pi(\mathbf{x},t_0)=\pi_0(\mathbf{x}), \quad \theta(\mathbf{x},t_0)=\theta_0(\mathbf{x}) \tag{24}$$

and boundary conditions

$$u=v=w=\theta=0 \quad \text{on} \quad z=0,1. \tag{25}$$

In the sequel, we will suppose that the $\mathbf{u}$, $\pi$ and $\theta$ are periodic functions in $x$ and $y$ direction, of period $\frac{2\pi}{a_x}$ and $\frac{2\pi}{a_y}$ respectively, and denote by

$$V=\left[0,\frac{2\pi}{a_x}\right]\times\left[0,\frac{2\pi}{a_y}\right]\times[0,1] \tag{26}$$

the periodicity cell. Finally, we will denote by $\langle\,,\,\rangle$ and $\|\,\|$ the usual scalar product and the related norm, respectively, of the Lebesgue space $L^2(V,\mathbb{C})$.

## 3. Instability analysis of $m_b$

In order to investigate the linear instability of (21) let us consider the linear version of system (23)

$$\begin{cases} \mathbf{u}=-\nabla\pi-\mathsf{Ra}M(z)\theta\mathbf{r}, \\ \nabla\cdot\mathbf{u}=0, \\ \frac{\partial\theta}{\partial t}+v_b(z)\theta_x+w=\Delta\theta. \end{cases} \tag{27}$$

By taking the third component of the double curl of $(27)_1$, one easily obtains

$$\begin{cases} \Delta w=\mathsf{Ra}\Big[-\sin\varphi\theta_x+M(z)\sin\varphi\theta_{xz}-\cos\varphi M(z)\Delta_1\theta\Big], \\ \dfrac{\partial\theta}{\partial t}+v_b(z)\theta_x+w=\Delta\theta. \end{cases} \tag{28}$$

Now by virtue of the periodicity and the fact that the system is linear and autonomous, we are allowed to seek (normal mode) solutions of the form (see [4,44–46])

$$w(\mathbf{x},t)=e^{i(a_xx+a_yy)}\widetilde{W}(z)e^{\sigma t} \quad \text{and} \quad \theta(\mathbf{x},t)=e^{i(a_xx+a_yy)}\widetilde{\Theta}(z)e^{\sigma t}, \tag{29}$$

with $\sigma \in \mathbb{C}$. By virtue of (29), (28) becomes

$$\begin{cases} (D^2 - a^2)\widetilde{W} = \mathrm{Ra}\left[-\sin\varphi i a_x \widetilde{\Theta} + (\zeta - z)\sin\varphi i a_x D\widetilde{\Theta} + (\zeta - z)\cos\varphi a^2 \widetilde{\Theta}\right], \\ (D^2 - a^2 - \sigma)\widetilde{\Theta} - \widetilde{W} = -\mathrm{Ra}\left(\zeta z - \frac{z^2}{2}\right)\sin\varphi i a_x \widetilde{\Theta}, \end{cases} \tag{30}$$

where $D = \frac{d}{dz}$, together with boundary conditions $\widetilde{W} = \widetilde{\Theta} = 0$, on $z = 0, 1$.

### 3.1. Analysis of the longitudinal perturbations

If we assume that the perturbations are longitudinal this means that they do not depend on $x$ and from (30) we obtain

$$\begin{cases} (D^2 - a_y^2)\widetilde{W} = \mathrm{Ra}(\zeta - z)\cos\varphi a_y^2 \widetilde{\Theta}, \\ (D^2 - a_y^2 - \sigma)\widetilde{\Theta} - \widetilde{W} = 0. \end{cases} \tag{31}$$

It is not difficult to show that $\sigma$ is a real number. Indeed, from $(31)_2$, one has

$$(D^2 - a_y^2)^2\widetilde{\Theta} - \sigma(D^2 - a_y^2)\widetilde{\Theta} - (D^2 - a_y^2)\widetilde{W} = 0, \tag{32}$$

then, from $(31)_1$, one gets

$$(D^2 - a_y^2)^2\widetilde{\Theta} - \sigma(D^2 - a_y^2)\widetilde{\Theta} - \mathrm{Ra}(\zeta - z)\cos\varphi a_y^2 \widetilde{\Theta} = 0. \tag{33}$$

Multiplying (33) by the complex conjugate of $\widetilde{\Theta}$ and integrating on the periodicity cell $V$, one obtains

$$\begin{aligned} \sigma\left(\int_0^1 (D\widetilde{\Theta})^2 dz + a_y^2 \int_0^1 \widetilde{\Theta}^2 dz\right) = &-\int_0^1 (D^2\widetilde{\Theta})^2 dz \\ &- 2a_y^2 \int_0^1 (D\widetilde{\Theta})^2 dz - a_y^4 \int_0^1 \widetilde{\Theta}^2 dz + \mathrm{Ra}\cos\varphi a_y^2 \int_0^1 (\zeta - z)\widetilde{\Theta}^2 dz. \end{aligned} \tag{34}$$

This shows that $\sigma \in \mathbb{R}$ and the principle of exchange of stability holds, i.e. convection can occur only via a stationary motion. As a consequence, we can set $\sigma = 0$ in (31)

$$\begin{cases} (D^2 - a_y^2)\widetilde{W} = \mathrm{Ra}(\zeta - z)\cos\varphi a_y^2 \widetilde{\Theta}, \\ (D^2 - a_y^2)\widetilde{\Theta} - \widetilde{W} = 0, \end{cases} \tag{35}$$

in order to find the critical linear Rayleigh number for the onset of stationary convective motions with respect to the longitudinal perturbations, for any fixed inclination angle and upper layer temperature:

$$\mathrm{Ra}_L^{\mathcal{L}} = \min_{a_y^2 \in \mathbb{R}^+} \mathrm{Ra}(a_y^2), \tag{36}$$

where the superscript $\mathcal{L}$ stays for Longitudinal. Moreover, it turns out that:

$$\mathrm{Ra}_L^{\mathcal{L}}(\varphi) = \frac{\mathrm{Ra}_L(0)}{\cos\varphi}, \tag{37}$$

with $\mathrm{Ra}_L(0)$ the critical linear Rayleigh number in the case of a horizontal layer $\varphi = 0$, see [16].

### 3.2. Analysis of the transverse perturbations

The system of transverse perturbations, i.e. independent on $y$, is introduced in this Section. Setting $a_y = 0$ in (30) one obtains:

$$\begin{cases} (D^2 - a_x^2)\widetilde{W} = \mathrm{Ra}\left[-\sin\varphi i a_x \widetilde{\Theta} + (\zeta - z)\sin\varphi i a_x D\widetilde{\Theta} + (\zeta - z)\cos\varphi a_x^2 \widetilde{\Theta}\right], \\ (D^2 - a_x^2 - \sigma)\widetilde{\Theta} - \widetilde{W} = -\mathrm{Ra}\left(\zeta z - \frac{z^2}{2}\right)\sin\varphi i a_x \widetilde{\Theta}. \end{cases} \tag{38}$$

It is worth observing that system (38) constitutes an eigenvalue system of ordinary differential equations

$$A\mathbf{x} = \sigma B\mathbf{x}, \tag{39}$$

with

$$A = \begin{pmatrix} D^2 - a_x^2 & \mathrm{Ra}\sin\varphi i a_x - \mathrm{Ra}(\zeta - z)\sin\varphi i a_x D \\ & -\mathrm{Ra}(\zeta - z)\cos\varphi a_x^2 \\ -I & D^2 - a_x^2 + \mathrm{Ra}\left(\zeta z - \frac{z^2}{2}\right)\sin\varphi i a_x \end{pmatrix} \tag{40}$$

and

$$B = \begin{pmatrix} 0 & 0 \\ 0 & I \end{pmatrix}. \tag{41}$$

The determination of the critical linear Rayleigh numbers with respect to the transverse perturbations, $\mathrm{Ra}_L^{\mathcal{T}}$ (where the superscript $\mathcal{T}$ stays for Transverse), and the related stability results are delegated to Section 6. In particular, the numerical method employed for the resolution of the generalized eigenvalue problem (39) is described in Section 5.

## 4. Nonlinear stability

In this Section, we perform the nonlinear stability analysis by applying the weighted energy method, see [47], to the system for nonlinear longitudinal perturbations in order to obtain the critical energy Rayleigh numbers from a maximum problem. Let us consider the system for nonlinear longitudinal perturbations

$$\begin{cases} u = -\mathrm{Ra}M(z)\theta\sin\varphi + \frac{\mathrm{Ra}}{2}\theta^2\sin\varphi \\ v = -\pi_y \\ w = -\pi_z - \mathrm{Ra}M(z)\theta\cos\varphi + \frac{\mathrm{Ra}}{2}\theta^2\cos\varphi \\ v_y + w_z = 0 \\ \theta_t + w + v\theta_y + w\theta_z = \Delta\theta \end{cases} \tag{42}$$

in particular we can reduce to study subsystem $(42)_{2-5}$, see [27]. Multiplying $(42)_2$ by $v$, $(42)_3$ by $w$, integrate each over $V$ and adding the result, one obtains

$$\|w\|^2 = -\mathrm{Ra}\cos\varphi\,\langle M(z)\theta, w\rangle + \frac{\mathrm{Ra}\cos\varphi}{2}\left\langle w, \theta^2\right\rangle, \tag{43}$$

and similarly, multiplying $(42)_5$ by $g(z)\theta$ (setting $g(z) = \mathrm{Ra}\cos\varphi(\mu - z)$ in order to get rid of the cubic nonlinear terms, with $\mu > 1$ being a coupling parameter) and integrating each, one obtains, adding the result with (43):

$$\begin{aligned} \frac{\mathrm{Ra}\cos\varphi}{2}\frac{d}{dt}\left\langle \mu - z, \theta^2\right\rangle = &-\|w\|^2 - \mathrm{Ra}\cos\varphi\,\langle(\mu + \zeta - 2z)\theta, w\rangle \\ &- \mathrm{Ra}\cos\varphi\left\langle \mu - z, |\nabla\theta|^2\right\rangle. \end{aligned} \tag{44}$$

Let us then consider the following weighted Lyapunov functional:

$$E(t) = \frac{\mathrm{Ra}\cos\varphi}{2}\left\langle \mu - z, \theta^2\right\rangle \tag{45}$$

and set

$$\begin{aligned} I(t) &= -\mathrm{Ra}\cos\varphi\,\langle(\mu + \zeta - 2z)\theta, w\rangle, \\ D(t) &= \|w\|^2 + \mathrm{Ra}\cos\varphi\left\langle \mu - z, |\nabla\theta|^2\right\rangle. \end{aligned} \tag{46}$$

Therefore, from (44) it follows that

$$\frac{dE}{dt} = I - D \le D(m - 1), \tag{47}$$

where

$$m = \max_{\mathcal{H}} \frac{I}{D}, \tag{48}$$

and $\mathcal{H}$ is the space of kinematically admissible perturbations, namely

$$\mathcal{H} = \left\{(w,\theta) \in [W^{1,2}(V)]^2 \mid w = \theta = 0 \text{ on } z = 0,1,\ w_z = 0,\right.$$
$$\left.\text{periodic in } y \text{ direction with period } 2\pi/a_y\right\}. \tag{49}$$

From Poincaré and weighted Poincaré inequalities, one obtains, see [47]

$$\frac{1}{2}\left\langle \mu - z, \theta^2 \right\rangle \leq \xi \left\langle \mu - z, |\nabla\theta|^2 \right\rangle, \tag{50}$$

where $\xi = \max\left\{\frac{c_p}{2}, 2\right\}$, and $c_p = c_p(V)$ is the Poincaré constant and, as a consequence, $D \geq \xi^{-1}E$. Hence, if $m < 1$ from (47) it follows

$$\frac{dE}{dt} \leq D(m-1) \leq \xi^{-1}(m-1)E, \tag{51}$$

i.e.

$$E(t) \leq E(0)\exp\left(\xi^{-1}(m-1)t\right). \tag{52}$$

The energy estimate (52) proves that, provided $m < 1$, $E$ decreases at least exponentially to zero as time goes to infinity. Finally, by using the generalized Cauchy-Schwartz and triangular inequalities we have

$$\left(1 - \frac{1}{2\varepsilon_1} - \frac{\varepsilon_2}{2}\right)\|w\|^2 \leq \mathrm{Ra}^2\cos^2\varphi\left(\frac{\varepsilon_1}{2}\|\theta\|^2 + \frac{1}{8\varepsilon_2}\|\theta^2\|^2\right), \tag{53}$$

and setting $\varepsilon_1 = 2$ and $\varepsilon_2 = \frac{1}{2}$, we get

$$\frac{1}{2}\|w\|^2 \leq \mathrm{Ra}^2\cos^2\varphi\left(\|\theta\|^2 + \frac{1}{4}\|\theta^2\|^2\right). \tag{54}$$

Estimate (54) implies that the condition $m < 1$ guarantees the exponential decay of the third component of the perturbed seepage velocity and the global nonlinear stability of the conduction solution with respect to the $E$-norm (45) is provided.

Concerning the variational problem (48) the associated Euler-Lagrange equations are the following

$$\begin{cases} 2mw\mathbf{k} + \mathrm{Ra}\cos\varphi(\mu + \zeta - 2z)\theta\mathbf{k} = \nabla\varpi \\ -(\mu + \zeta - 2x)w - m\theta_z + m(\mu - z)\Delta\theta = 0 \end{cases} \tag{55}$$

where $\varpi$ is a Lagrange multiplier. Let us remark that the nonlinear stability condition $m < 1$ is equivalent to the condition $\mathrm{Ra} < \mathrm{Ra}_E$, where $\mathrm{Ra}_E$ is the critical nonlinear Rayleigh number. Therefore, the criticality is reached when $\mathrm{Ra} = \mathrm{Ra}_E$ in system (55) in correspondence of $m = 1$. Therefore, taking the third component of the double curl of $(55)_1$ and employing normal modes representation in (55), we obtain:

$$\begin{cases} (D^2 - a_y^2)W - \mathrm{Ra}\cos\varphi\left(\frac{\mu}{2} + \frac{\zeta}{2} - z\right)a_y^2\Theta = 0 \\ \left(\frac{\mu}{2} + \frac{\zeta}{2} - z\right)W + D\Theta - (\mu - z)(D^2 - a_y^2)\Theta = 0 \end{cases} \tag{56}$$

together with boundary conditions $W = \Theta = 0$, on $z = 0, 1$. System (56) is a fourth-order generalized eigenvalue problem for the critical Rayleigh number $\mathrm{Ra}_E$, which is given by

$$\mathrm{Ra}_E^{\mathcal{L}} = \max_{\mu > 1}\min_{a^2 \in \mathbb{R}^+}\mathrm{Ra}(a_y^2, \mu) \tag{57}$$

Moreover, it turns out that:

$$\mathrm{Ra}_E^{\mathcal{L}}(\varphi) = \frac{\mathrm{Ra}_E(0)}{\cos\varphi}, \tag{58}$$

with $\mathrm{Ra}_E(0)$ the critical non-linear Rayleigh number in the case of a horizontal layer $\varphi = 0$, see [16].

## 5. Numerical method

In this section the eigenvalue system (39)-(41) is solved using the Chebyschev-$\tau$ method developed by Dongarra et al in [48]. In order to ensure a deeper comprehensibility and repeatability of the employed method, let us start by considering the following generalized eigenvalue problem with homogeneous boundary conditions

$$\begin{cases} Lu(x) = \sigma M u(x) & x \in [-1,1] \\ B_1 u(1) = 0 & C_1 u(-1) = 0 \\ \vdots & \vdots \\ B_{\frac{\Gamma}{2}} u(1) = 0 & C_{\frac{\Gamma}{2}} u(-1) = 0 \end{cases} \tag{59}$$

where $L$ and $M$ are two arbitrary differential operators of order $\Gamma$, and $B_i$, $C_i$ are the operators defining the set of boundary conditions at $x = 1$ and $x = -1$, respectively.

On multiplying the equation and the boundary conditions in (59) by the $i$-th $(i = 0, \ldots, N)$ Chebyschev polynomial under the usual product $\int_{-1}^{1} f(x)g(x)\frac{dx}{\sqrt{1-x^2}}$, one obtains:

$$\sum_{k=0}^{N}\sum_{j=0}^{N+\Gamma} L_{kj}u_j = \sigma\sum_{k=0}^{N}\sum_{j=0}^{N+\Gamma} M_{kj}u_j, \tag{60}$$

$$\begin{aligned} Bu(1) = 0 \quad &\Rightarrow \sum_{k=0}^{N+\Gamma}\sum_{j=0}^{N+\Gamma} B_{kj}u_j = 0, \\ Cu(-1) = 0 \quad &\Rightarrow \sum_{k=0}^{N+\Gamma}\sum_{j=0}^{N+\Gamma} (-1)^k C_{kj}u_j = 0. \end{aligned} \tag{61}$$

Therefore, the system can be written as

$$\begin{pmatrix} L \\ \mathbf{b}_i^T \\ \mathbf{c}_i^T \end{pmatrix}\mathbf{u} = \sigma\begin{pmatrix} M \\ \mathbf{0}_i^T \\ \mathbf{0}_i^T \end{pmatrix}\mathbf{u}. \tag{62}$$

Since the boundary conditions establish a relation between the last $\Gamma$ coefficients and the others, the last $\Gamma$ rows of the left-side matrix can be used to erase the last $\Gamma$ columns of the first $N+1$ row of the matrices belonging to the right and left side of the equation. The following form is now obtained

$$\begin{pmatrix} L' & 0 & \ldots & 0 \\ & \mathbf{b}_i^T & & \\ & \mathbf{c}_i^T & & \end{pmatrix}\mathbf{u} = \sigma\begin{pmatrix} M' & 0 & \ldots & 0 \\ & \mathbf{0}_i^T & & \\ & \mathbf{0}_i^T & & \end{pmatrix}\mathbf{u}, \tag{63}$$

where $L'$ and $M'$ are the operator matrices after this reduction. The equation can be now limited to the first $N+1$ coefficient

$$L'\mathbf{u}' = \sigma M'\mathbf{u}', \tag{64}$$

where $\mathbf{u}'$ is the vector containing the first $N+1$ expansion coefficients. Since the matrix $M'$ is not singular, the problem can be reduced to a standard eigenvalue problem and it can be solved with standard methods.

In order to apply the above method to the eigenvalue problem (39)-(41), the equations and the boundary conditions need to be changed into a suitable framework. With this aim, applying the $\left(D^2 - a^2\right)$ operator to $(30)_2$ we obtain

$$\begin{aligned} \left(D^2 - a^2\right)\widetilde{W} = \left(D^2 - a^2\right)^2\widetilde{\Theta} - \sigma\left(D^2 - a^2\right)\widetilde{\Theta} \\ + \mathrm{Ra}\sin\varphi i a_x\left[\left(\zeta z - \frac{z^2}{2}\right)\left(D^2 - a^2\right) + 2(\zeta - z)D - 1\right]\widetilde{\Theta}, \end{aligned} \tag{65}$$

and, substituting it into $(30)_1$, we get

$$\begin{aligned} \left\{\left(D^2 - a^2\right)^2 + \mathrm{Ra}\sin\varphi i a_x\left[\left(\zeta z - \frac{z^2}{2}\right)\left(D^2 - a^2\right)\right.\right. \\ \left.\left. + (\zeta - z)D\right] - \mathrm{Ra}\cos\varphi a^2\right\}\widetilde{\Theta} = \sigma\left(D^2 - a^2\right)\widetilde{\Theta}. \end{aligned} \tag{66}$$

Let us notice that, in order to change the boundaries from $[0,1]$ to $[-1,1]$ the change of variable $z = \frac{\hat{z}}{2} + \frac{1}{2}$ is performed. Then, defining $\widehat{\mathrm{Ra}} = \frac{\mathrm{Ra}}{4}$, $\hat{a}_x = \frac{a_x}{2}$, $\hat{a}_y = \frac{a_y}{2}$, $\hat{D} = \frac{d}{d\hat{z}}$, we have

**Table 1**
Critical Rayleigh numbers for quoted values of the upper layer temperature and inclination angles.

| $\zeta = 1\,(T_U = 4)$ | | | $\zeta \simeq 0.6\,(T_U = 6)$ | | | $\zeta = 0.5\,(T_U = 8)$ | | | |
|---|---|---|---|---|---|---|---|---|---|
| $\mathrm{Ra}_E^{\mathcal{L}}$ | $\mathrm{Ra}_L^{\mathcal{L}}$ | $\mathrm{Ra}_L^{\mathcal{T}}$ | $\mathrm{Ra}_E^{\mathcal{L}}$ | $\mathrm{Ra}_L^{\mathcal{L}}$ | $\mathrm{Ra}_L^{\mathcal{T}}$ | $\mathrm{Ra}_E^{\mathcal{L}}$ | $\mathrm{Ra}_L^{\mathcal{L}}$ | $\mathrm{Ra}_L^{\mathcal{T}}$ | $\varphi(deg)$ |
| 74.219 | 77.0797 | 77.0797 | 154.873 | 198.031 | 198.031 | 248.009 | 471.483 | 471.483 | 0 |
| 74.502 | 77.3741 | 77.8129 | 155.464 | 199.7874 | 199.617 | 248.956 | 473.284 | 475.651 | 5 |
| 75.364 | 78.2687 | 80.1363 | 157.262 | 201.0859 | 205.441 | 251.835 | 478.756 | 488.752 | 10 |
| 76.837 | 79.7987 | 84.4853 | 160.336 | 205.0167 | 215.832 | 256.758 | 488.115 | 512.864 | 15 |
| 78.982 | 82.0265 | 91.8193 | 164.812 | 210.7402 | 233.725 | 263.956 | 501.742 | 552.685 | 20 |
| 81.891 | 85.04804 | 104.945 | 170.883 | 218.5030 | 261.563 | 273.648 | 520.224 | 618.801 | 25 |
| 85.701 | 89.0039 | 135.478 | 178.832 | 228.6665 | 317.971 | 286.376 | 544.422 | 742.793 | 30 |
| 90.605 | 94.0969 | * | 189.065 | 241.7512 | 511.990 | 302.763 | 575.574 | 1115.460 | 35 |

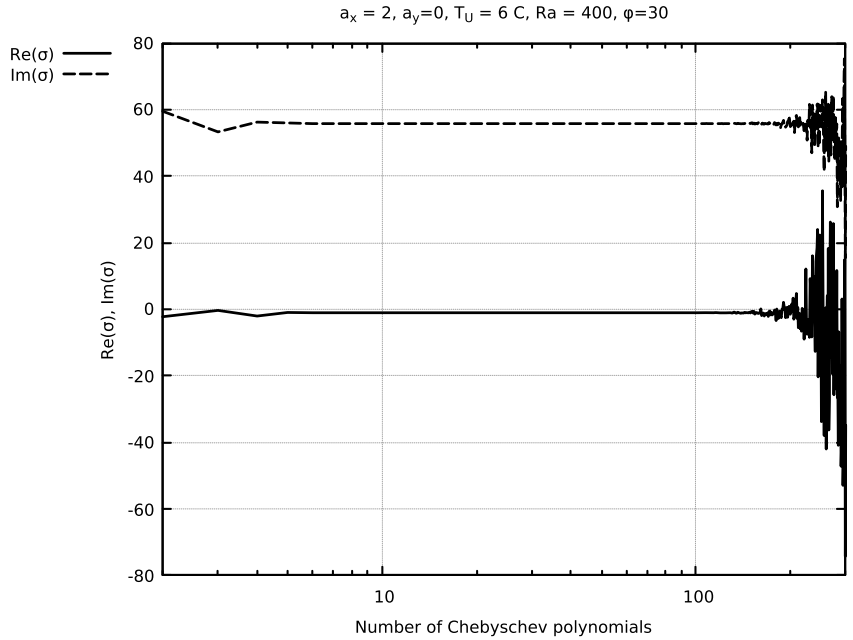


**Fig. 1.** Sensitivity of eigenvalue calculations on number of polynomials.

$$\begin{cases} L\widetilde{\Theta} = \sigma\left(\widehat{D}^2 - \widehat{a}^2\right)\widetilde{\Theta} \\ \widetilde{\Theta}(z) = 0, \quad z = \pm 1, \\ \widehat{D}^2\widetilde{\Theta}(z) = 0, \quad z = \pm 1, \end{cases} \tag{67}$$

with

$$L = \left(\widehat{D}^2 - \widehat{a}^2\right) + \widehat{\mathrm{Ra}}\sin\varphi i\widehat{a}_x\left[P_2(\widehat{z})\left(\widehat{D}^2 - \widehat{a}^2\right) + P_1(\widehat{z})\widehat{D}\right] - \widehat{\mathrm{Ra}}\cos\varphi\widehat{a}^2, \tag{68}$$

where we set

$$P_1(\widehat{z}) = \zeta(\widehat{z}+1) - \frac{(\widehat{z}+1)^2}{4}, \quad P_2(\widehat{z}) = \zeta(\widehat{z}+1) - \frac{\widehat{z}+1}{2}. \tag{69}$$

Since the problem has been reduced to a form like (59) the method can be employed in order to find the eigenvalues through Shur's decomposition. Indeed, in the spectrum of the found eigenvalues the one with the largest real part is selected, and, for every fixed wave number, the Rayleigh number is varied until its real part changes its sign. The range of the Rayleigh number and wave number has been chosen for the purpose of individuating the locus of the minimum of the marginal stability curve. This sign changing from negative(positive) to positive(negative) marks the transition from stability(instability) to instability(stability). The calculation has been then repeated for different inclination angles until none of this kind of point is found. This procedure has been repeated for several temperature values of the upper layer, $T_U = 4, 6, 8\ ^\circ C$ as long as we want to investigate penetrative convection in the parabolic neighborhood of the maximum density value. The linear critical Rayleigh numbers with respect to the transverse perturbations are reported in Table 1.

In conclusion, let us report that a preliminary study of the method's performance has been conducted. First of all, a sensitivity analysis has been conducted to investigate the behavior of the solver on the employed number of polynomials. Moreover, simulations with different numbers of polynomials have been launched calculating the eigenvalues of the investigated equation for the following parameters:

$$T_U = 4^\circ C, \quad a_x = 2, \quad a_y = 0, \quad \mathrm{Ra} = 400, \quad \phi = 30^\circ$$

The results are shown in Fig. 1: the values of both imaginary and real part of the calculated most unstable eigenvalues are stable for a number of polynomials between 8 and 120. This kind of analysis is the same conducted by Orszag [49], showing the convergence of the Chebyschev $\tau$-method for the penetrative convection problem discussed above. With a larger number of polynomials, the results are strongly unstable. This is due to the truncation error in the derivative matrices as stressed by Dongarra et al. [48]. From this analysis, the choice of 16 polynomials to perform the calculations seemed reasonable, ensuring desired precision and avoiding truncation errors and time-consuming simulations.

## 6. Numerical results and conclusions

In this section, we present the results from the numerical solution of the generalized eigenvalue problems (35), (38) and (56), arising from the linear analysis of longitudinal and transverse perturbations and the non-linear analysis of the longitudinal perturbations, respectively. To

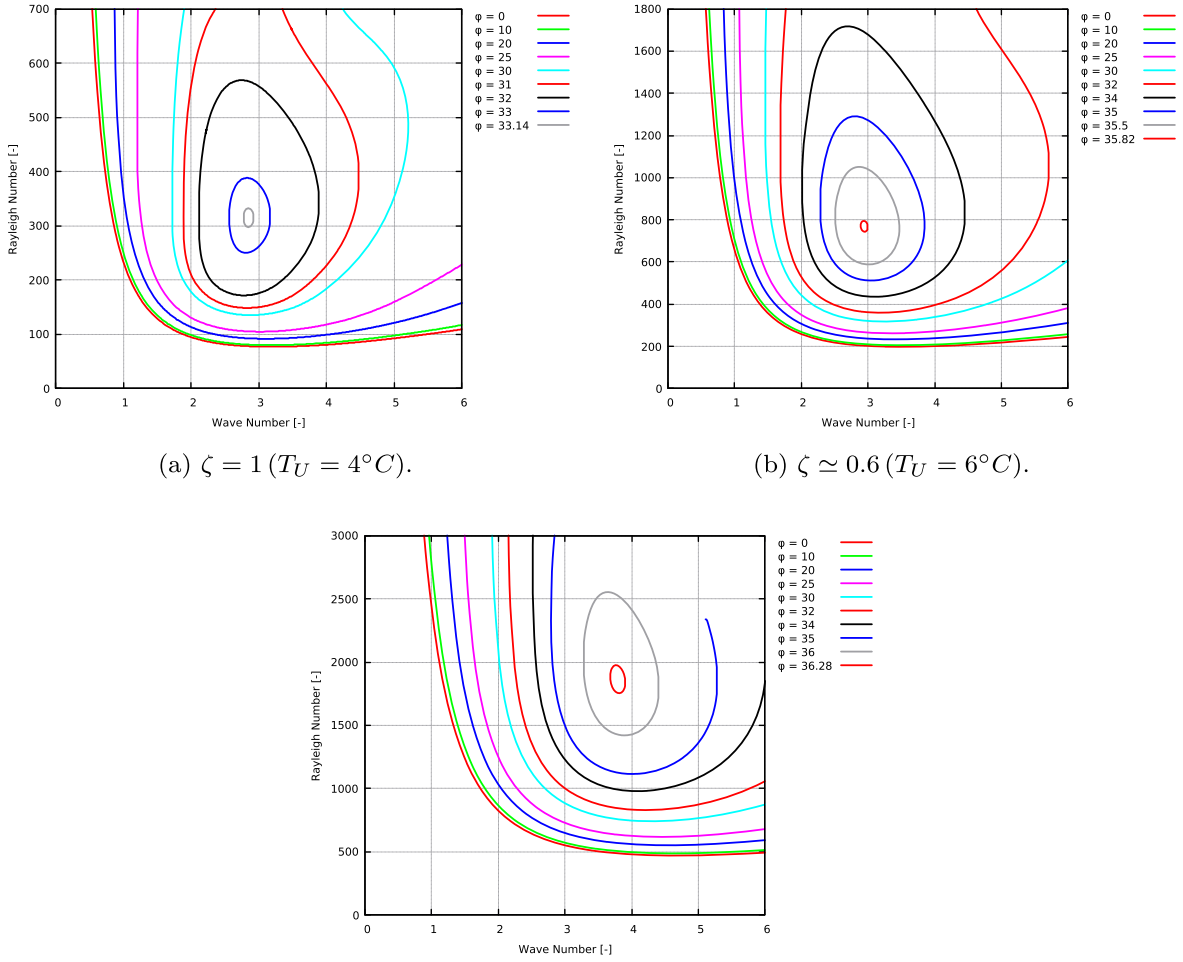


(a) $\zeta = 1\,(T_U = 4°C)$. (b) $\zeta \simeq 0.6\,(T_U = 6°C)$.

(c) $\zeta = 0.5\,(T_U = 8°C)$.

**Fig. 2.** Marginal stability curves for quoted values of the upper layer temperature, related to the linear transverse perturbations.

evaluate the effect of the layer inclination and of the upper-layer temperature on the onset of convective motions, we performed numerical simulations for quoted values of $\varphi$ and $T_U$, respectively.

Concerning the linear analysis of the transverse perturbations, in Fig. 2 we can observe the marginal stability curves for quoted values of the layer inclination and the upper-layer temperature, and the corresponding critical Rayleigh numbers are reported in Table 1. These curves are obtained by selecting, for a fixed wave number, the linear Rayleigh number at which the real part of the eigenvalue changes its sign. Fig. 2 shows clearly the stabilizing effect of inclination on the onset of penetrative convection. Moreover, regarding the upper-layer temperature, we can observe that:

- since $\zeta = \dfrac{T_0}{T_U}$, with $T_0 = 4°C$, is inversely proportional to the temperature of the upper layer, as the temperature of the upper layer increases, given a fixed inclination, instabilities arise at a higher Rayleigh number, showing the stabilizing effect of the upper layer temperature;
- on the other hand, higher temperature allows instability to arise at higher inclination.

The latter behavior can be seen in a clearer way in Fig. 3 (a), where the critical Rayleigh numbers are plotted against the inclination at different temperatures. The continuous lines represent the critical Rayleigh numbers for longitudinal perturbations while the dashed ones represent the transverse ones. It can be noticed that the transversal perturbations are more stable than the longitudinal ones for *all* the inclinations. Moreover, temperature increases shift to higher values of the critical angle as it is shown in Table 2.

**Table 2**
Critical values of $\varphi$.

| | $\zeta = 1\,(T_U = 4)$ | $\zeta \simeq 0.6\,(T_U = 6)$ | $\zeta = 0.5\,(T_U = 8)$ |
|---|---|---|---|
| $\varphi_{cr}$ | 33.16° | 35.84° | 36.30° |

Let us remark that, as it is expected, in the case of a horizontal layer, i.e. $\varphi = 0$, the found critical thresholds coincide with the ones found in [16].

Moreover, from the analysis of the three-dimensional perturbations, see e.g. Fig. 4, we saw that the longitudinal perturbations are the most destabilizing not only with respect to the transversal perturbations but also with respect to any rolls in the plane $(a_x, a_y)$, proving a Squire-like theorem for the problem under examination. Lastly, nonlinear analysis of longitudinal perturbations has been performed with the weighted energy method and in Fig. 3(b) the critical thresholds are plotted against inclinations for quoted values of upper layer temperature, comparing them for the corresponding threshold obtained through the linear analysis.

In summary, our results show that:

- in the limit case $\varphi \to 0$, i.e. horizontal layers, the instability thresholds coincide with the ones found in [16], [32, pag. 383] and [50];

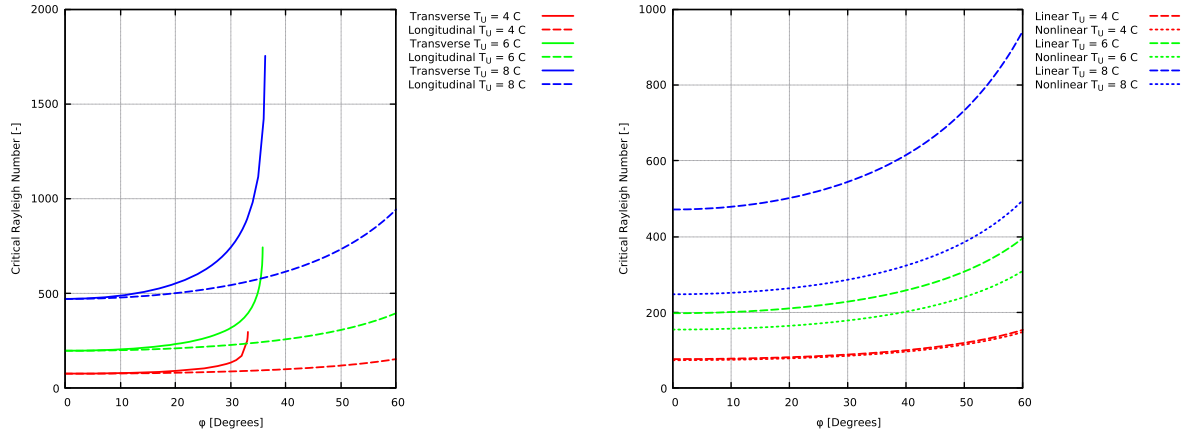


(a) Critical longitudinal and transverse Rayleigh numbers as functions of the layer's inclination.

(b) Critical linear and non-linear longitudinal Rayleigh numbers as functions of the layer's inclination.

**Fig. 3.** Comparison of marginal stability curves.

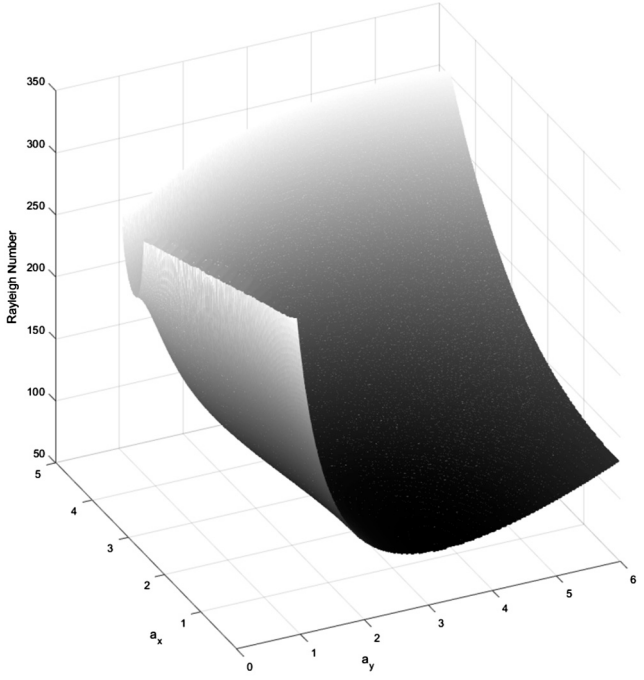


**Fig. 4.** Critical surface in correspondence of $\zeta = 1\,(T_U = 4°C)$ and $\varphi = 33°$.

- the inclination of the layer has a stabilizing effect on the onset of convection;
- the most destabilizing perturbations are the longitudinal ones;
- a Squire's-like theorem is numerically proved, which means that the longitudinal perturbations are the most dangerous with respect to any general roll perturbation;
- the principle of exchange of stabilities has been proved in the case of longitudinal perturbations;
- the transverse perturbations destabilize only up to a certain inclination's angle and the critical angles are found for quoted values of the upper plane temperature;
- the nonlinear stability analysis for the longitudinal perturbations, with the weighted energy method, is performed.

## CRediT authorship contribution statement

**Giuseppe Arnone:** Conceptualization, Formal analysis, Investigation, Methodology, Visualization, Writing – original draft, Writing – review & editing. **Giulio Cantini:** Conceptualization, Formal analysis, Investigation, Methodology, Visualization, Writing – original draft, Writing – review & editing. **Florinda Capone:** Conceptualization, Formal analysis, Investigation, Methodology, Visualization, Writing – original draft, Writing – review & editing. **Mauro Carnevale:** Conceptualization, Formal analysis, Investigation, Methodology, Visualization, Writing – original draft, Writing – review & editing.

## Declaration of competing interest

The authors declare that they have no known competing financial interests or personal relationships that could have appeared to influence the work reported in this paper.

## Data availability

No data was used for the research described in the article.

## Acknowledgements

This paper has been performed under the auspices of the National Group of Mathematical Physics (GNFM-INdAM). G. Arnone would like to thank Progetto Giovani GNFM 2023: "Modelli per la propagazione termica governati dalla legge di Darcy frazionaria", CUP_E53C22001930001. The authors want to thank Simon Vella for his expertise in helping them to present the 3D numerical simulations with high-quality images and Jacopo Gianfrani for his helpful suggestions. The authors kindly thank the anonymous Referees, whose suggestions and comments led to significant improvements in the manuscript.

## References

[1] A.V. Getling, Rayleigh-Bénard Convection: Structures and Dynamics, vol. 11, World Scientific, 1998.
[2] D.A. Nield, A. Bejan, Convection in Porous Media, Springer, 2017.
[3] R. de Boer, Theory of Porous Media, Highlights in Historical Development and Current State, Springer, 2000.
[4] S. Chandrasekhar, Hydrodynamic and Hydromagnetic Stability, Dover, 1981.
[5] H. Bénard, Les tourbillon cellulaires dans une nappe liquide, Revue Gan. Sci. Pur. Appl. 11 (1900).

[6] J.W. Strutt, On convection currents in a horizontal layer of fluid, when the higher temperature is on the under side, Philos. Mag. 32 (1916) 529–546.
[7] C.W. Horton, F.T. Rogers, Convection currents in a porous medium, J. Appl. Phys. 16 (1945) 367–370.
[8] E.R. Lapwood, Convection of a fluid in a porous medium, Math. Proc. Camb. Philos. Soc. 44 (1948) 508–521.
[9] R. Wooding, Rayleigh instability of a thermal boundary layer in flow through a porous medium, J. Fluid Mech. 9 (2) (1960) 183–192.
[10] J.W. Elder, Steady free convection in a porous medium heated from below, J. Fluid Mech. 27 (1) (1967) 29–48.
[11] A. Mahidjiba, L. Robilland, P. Vasseur, Onset of penetrative convection of cold water in a porous layer under mixed boundary conditions, Int. J. Heat Mass Transf. 49 (2006) 2820–2828.
[12] G. Veronis, Penetrative convection, Astrophys. J. 137 (1963) 641–663.
[13] B. Straughan, Finite amplitude instability thresholds in penetrative convection, Geophys. Astrophys. Fluid Dyn. 34 (1–4) (1984) 227–242.
[14] D. Lyubimov, T. Lyubimova, V. Sharifulin, Onset of convection in a horizontal fluid layer in the presence of density inversion under given heat fluxes at its boundaries, Fluid Dyn. 47 (4) (2012) 448–453.
[15] F. Capone, M. Gentile, A.A. Hill, Penetrative convection in anisotropic porous media with variable permeability, Acta Mech. 216 (2011) 49–58.
[16] G. Arnone, F. Capone, Density inversion phenomenon in porous penetrative convection, Int. J. Non-Linear Mech. (2022) 104198.
[17] J.H. George, R.D. Gunn, B. Straughan, Patterned ground formation and penetrative convection in porous media, Geophys. Astrophys. Fluid Dyn. 46 (1989) 135–158.
[18] K. Hutter, B. Straughan, Penetrative convection in thawing subsea permafrost, Contin. Mech. Thermodyn. 9 (1997) 259–272.
[19] H. Inaba, M. Sugawara, J. Blumenberg, Natural convection heat transfer in an inclined porous layer, Int. J. Heat Mass Transf. 31 (7) (1988) 1365–1374.
[20] A.W. Woods, S.J. Linz, Natural convection and dispersion in a tilted fracture, J. Fluid Mech. 241 (1992) 59–74.
[21] P. Falsaperla, G. Mulone, B. Straughan, Bidispersive-inclined convection, Proc. R. Soc. A, Math. Phys. Eng. Sci. 472 (2192) (2016) 20160480.
[22] T. Kaneko, M. Mohtadi, K. Aziz, An experimental study of natural convection in inclined porous media, Int. J. Heat Mass Transf. 17 (4) (1974) 485–496.
[23] B. Kamkari, H. Shokouhmand, F. Bruno, Experimental investigation of the effect of inclination angle on convection-driven melting of phase change material in a rectangular enclosure, Int. J. Heat Mass Transf. 72 (2014) 186–200.
[24] D.A.S. Rees, A. Bassom, The onset of Darcy-Bénard convection in an inclined layer heated from below, Acta Mech. 144 (2000) 103–118.
[25] A. Barletta, L. Storesletten, Thermoconvective instabilities in an inclined porous channel heated from below, Int. J. Heat Mass Transf. 54 (13–14) (2011) 2724–2733.
[26] A. Barletta, M. Celli, The Horton–Rogers–Lapwood problem for an inclined porous layer with permeable boundaries, Proc. R. Soc. A, Math. Phys. Eng. Sci. 474 (2217) (2018) 20180021.
[27] P. Falsaperla, G. Mulone, Thermal convection in an inclined porous layer with Brinkman law, Ric. Mat. 67 (2018) 983–999.
[28] L. Storesletten, D.A.S. Rees, Onset of convection in an inclined anisotropic porous layer with internal heat generation, Fluids 4 (2) (2019) 75.
[29] P. Falsaperla, A. Giacobbe, G. Mulone, Inclined convection in a porous Brinkman layer: linear instability and nonlinear stability, Proc. R. Soc. A 475 (2223) (2019) 20180614.
[30] T. Lyubimova, I. Muratov, I. Shubenkov, Onset and nonlinear regimes of convection in an inclined porous layer subject to a vertical temperature gradient, Phys. Fluids 34 (9) (2022) 094114.
[31] B. Straughan, Stability and Wave Motion in Porous Media, Springer, 2008.
[32] B. Straughan, The Energy Method, Stability, and Nonlinear Convection, Springer, 2004.
[33] J.N. Flavin, S. Rionero, Qualitative Estimates for Partial Differential Equations: An Introduction, Taylor and Francis Inc, 1995.
[34] F. Capone, M. Gentile, G. Massa, The onset of thermal convection in anisotropic and rotating bidisperse porous media, Z. Angew. Math. Phys. 72 (2021) 169.
[35] F. Capone, J.A. Gianfrani, Onset of convection in LTNE Darcy–Brinkman anisotropic porous layer: Cattaneo effect in the solid, Int. J. Non-Linear Mech. 139 (2022).
[36] A. Giacobbe, G. Mulone, Stability in the rotating Bénard problem and its optimal Lyapunov functions, Acta Appl. Math. 132 (2014) 307–320.
[37] F. Capone, M. Gentile, Sharp stability results in LTNE rotating anisotropic porous layer, Int. J. Therm. Sci. 134 (2018) 661–664.
[38] A. Barletta, G. Mulone, The energy method analysis of the Darcy–Bénard problem with viscous dissipation, Contin. Mech. Thermodyn. 33 (2021) 25–33.
[39] H.B. Squire, On the stability for three-dimensional disturbances of viscous fluid flow between parallel walls, Proc. R. Soc. Lond. Ser. A, Contain. Pap. Math. Phys. Character 142 (847) (1933) 621–628.
[40] P.G. Drazin, W.H. Reid, Hydrodynamic Stability, Cambridge University Press, 2004.
[41] M.H. Allouche, S. Millet, V. Botton, D. Henry, H.B. Hadid, F. Rousset, Stability of a flow down an incline with respect to two-dimensional and three-dimensional disturbances for Newtonian and non-Newtonian fluids, Phys. Rev. E 92 (6) (2015) 063010.
[42] I. Müller, Thermodynamics, Pitman, London, 1985.
[43] H. Gouin, A. Muracchini, T. Ruggeri, On Müller paradox for thermal-incompressible media, Contin. Mech. Thermodyn. 24 (2011) 505–513.
[44] G.C. Rana, The onset of thermal convection in couple-stress fluid in hydromagnetics saturating a porous medium, Bull. Pol. Acad. Sci., Tech. Sci. (2014) 357–362.
[45] G. Rana, R. Chand, Stability analysis of double-diffusive convection of Rivlin-Ericksen elastico-viscous nanofluid saturating a porous medium: a revised model, Forsch. Ingenieurwes. 79 (1–2) (2015) 87–95.
[46] R. Chand, G. Rana, Thermal instability of Rivlin–Ericksen elastico-viscous nanofluid saturated by a porous medium, J. Fluids Eng. 134 (12) (2012).
[47] G.P. Galdi, S. Rionero, Weighted Energy Methods in Fluid Dynamics and Elasticity, Springer, 1995.
[48] J. Dongarra, B. Straughan, D. Walker, Chebyshev tau-QZ algorithm methods for calculating spectra of hydrodynamic stability problems, Appl. Numer. Math. 22 (1996) 399–434.
[49] S.A. Orszag, Accurate solution of the Orr–Sommerfeld stability equation, J. Fluid Mech. 50 (4) (1971) 689–703, https://doi.org/10.1017/S0022112071002842.
[50] A.A. Hill, S. Rionero, B. Straughan, Global stability for penetrative convection with throughflow in a porous material, IMA J. Appl. Math. 72 (2007) 635–643.